Published in final edited form as:

Heart Rhythm. 2019 April ; 16(4): 588–594. doi:10.1016/j.hrthm.2018.10.029.

Association of regional myocardial conduction velocity with the distribution of hypoattenuation on contrast-enhanced perfusion computed tomography in patients with post-infarct ventricular tachycardia

Tuna Ustunkaya, MD, PhD[a], **Benoit Desjardins, MD, PhD**[b], **Bolun Liu, MD**[a], **Sohail Zahid, PhD**[c], **Jaeseok Park, MD**[a], **Nissi Saju, RN**[d], **Natalia Trayanova, PhD, FHRS**[c], **Stefan L. Zimmerman, MD**[d], **Francis E. Marchlinski, MD, FHRS**[a], and **Saman Nazarian, MD, PhD, FHRS**[a]

[a]Cardiac Electrophysiology, Hospital of the University of Pennsylvania 3400 Spruce Street, Philadelphia, PA, 19103

[b]Cardiovascular Imaging, Hospital of the University of Pennsylvania 3400 Spruce Street, Philadelphia, PA 19103

[c]Biomedical Engineering, Johns Hopkins University 3400 University Drive, Baltimore, MD 21218

[d]Radiology, Johns Hopkins University School of Medicine 1800 Orleans Street, Baltimore, MD 21287

Abstract

Background: Cardiac magnetic resonance imaging has been shown to be beneficial for identification of the ventricular tachycardia (VT) substrate prior to catheter ablation. Contrast-enhanced perfusion multidetector CT (CEP-MDCT) is more generalizable to clinical practice; and wall thickness and regional hypoenhancement on CEP-MDCT can identify potential substrate sites, albeit with decreased specificity.

Objective: We sought to evaluate the association between wall thickness and attenuation on CEP-MDCT with local conduction velocity and electrogram abnormalities in patients with post-infarct VT.

Methods: 14 patients with post-infarct VT underwent pre-procedural CEP-MDCT followed by endocardial electroanatomical mapping (EAM) and ablation. Myocardial attenuation and wall thickness were calculated from 3D MDCT images using ADAS-VT software (Galgo Medical, Spain). EAM was registered with 3D-MDCT images using the CartoMERGE module of CARTO3

Corresponding author: Saman Nazarian MD, PhD, University of Pennsylvania Perelman School of Medicine, Division of Cardiac Electrophysiology, 3400 Spruce Street/Founders 9, Philadelphia, PA 19143, saman.nazarian@uphs.upenn.edu, Phone: +1 (215) 615-5220, Fax: + 1 (215) 615-5235.

The University of Pennsylvania Conflict of Interest Committee manages all commercial arrangements.

software (Biosense Webster Inc. Diamond, CA). Local conduction velocity was calculated by averaging the velocity between each point and 5 adjacent points with concordant wave-front direction.

Results: A total of 3689 points were included. In multivariable regression analysis clustered by patient, local conduction velocity was positively associated with myocardial attenuation, bipolar voltage, unipolar voltage, and wall thickness. Each 10 HU drop in full-thickness attenuation correlated to 2.6% decrease in conduction velocity ($p<0.001$) and 5.5% decrease in bipolar voltage amplitude ($p<0.001$), after adjusting for wall thickness.

Conclusion: The myocardial attenuation distribution on CEP-MDCT is associated with regional conduction velocity and electrogram amplitude. Regions with low conduction velocity identified with low attenuation on CEP-MDCT may serve as important VT substrates in post-infarct patients.

Keywords

conduction velocity; contrast enhanced computed tomography; ventricular tachycardia; ischemic cardiomyopathy; catheter ablation; hypoattenuation

Introduction

Sustained ventricular tachycardia (VT) is an important cause of post-myocardial infarction morbidity and mortality. Although antiarrhythmic drugs have been demonstrated to reduce VT burden, their utilization is limited by side effects and suboptimal efficacy. Radiofrequency catheter ablation (RFCA) of VT is an excellent alternative to medical therapy as a primary option or when antiarrhythmic drugs are ineffective or intolerable.[1] Electroanatomical mapping (EAM), an essential element of VT RFCA procedures, is often limited by poor sampling density in the setting of complex intramural anatomy, thrombi, or epicardial fat, as well as measurement bias due to suboptimal catheter contact. Techniques for integration or feature extraction from pre-procedural positron emission tomography (PET) or magnetic resonance (MRI) images improve substrate identification as an adjunct to EAM.[2, 3] However, PET is limited by spatial resolution and MRI suffers from poor generalizability due to safety and image quality issues related to implantable defibrillators.[4] Contrast-enhanced perfusion multi-detector computed tomography (CEP-MDCT) is generalizable to clinical practice, provides superior spatial resolution, and is a validated modality for scar identification following myocardial infarction.[5] Moreover, critical VT sites and abnormal substrates on EAM have been shown to associate with wall thickness, wall motion, fat deposition and hypoperfusion on CEP-MDCT.[6–9]

Myocardial conduction velocity (CV) heterogeneity, a common finding after extensive myocardial infarction, is a prerequisite for re-entrant VT. Previous studies have demonstrated that post-infarct patients with prevalent VT exhibit peri-infarct channels with lower local CV compared to those without VT.[10] Moreover, pharmacologic enhancement of CV reduces arrhythmogenicity in peri and post-infarct models.[11] Variations in individual patient coronary distribution, coronary stenosis location, wall thickness, coronary perfusion pressure, time to revascularization, pre-conditioning, and medication regime, result in significant inter-patient variations in the distribution of slow conduction substrates for VT.

The most critical reentrant circuit locations and those most vulnerable to limited ablation, are sites with slow conduction, thus understanding the association of natomic changes on CEP-MDCT with local CV may inform target selection for catheter ablation. In this study, we sought to examine the association of a) myocardial CEP-MDCT attenuation with local CV and electrogram amplitude and b) local CV with VT circuit sites.

Methods

Study Population

The Johns Hopkins University School of Medicine and the University of Pennsylvania Perelman Institutional Review Boards approved the study protocol. Fourteen patients with underlying post-infarct VT who underwent ventricular tachycardia ablation and mapping were prospectively enrolled. All patients provided written informed consent prior to undergoing pre-procedural CEP-MDCT, EAM, and VT ablation.

CEP-MDCT acquisition

CEP-MDCT images were obtained using a Toshiba Aquillion 320-slice multidetector CT system during breath hold to detect first pass perfusion. Bolus triggering based on attenuation in the descending aorta was utilized with image acquisition during mid-diastole (dFOV: 200–220, range: 128–140 mm, gantry rotation 0.275 ms, tube voltage 80–120 kV, tube current 310–700 mA). Contrast (Isovue-370 in 14, Visipaque in 1; 70–80 cc) was administered as (1) contrast injection (2) 50/50 contrast/saline injection and (3) saline flush. Images were reconstructed using myocardium-optimized reconstruction kernels including beam hardening artifact correction (thickness 0.5 –3 mm). Images acquired between 70–80% R-R interval were selected to minimize motion artifact.

Electroanatomic Mapping

Left ventricular EAM was performed using the CARTO3 system (Biosense Webster, Diamond Bar, CA) with 3.5 mm open-irrigated Thermocool SF catheter (Biosense Webster, Diamond Bar, CA) or with the multi-electrode PentaRAY catheter (Biosense Webster, Diamond Bar, CA) during baseline rhythm via a retrograde aortic or trans-septal approach depending upon physician preference. Endocardial contact during point acquisition was validated by recording of a stable contact signal for >2 beats. Local activation time was annotated relative to a sharp QRS deflection for each EAM point. Points acquired during ectopic beats with different intracardiac activation sequence or QRS morphology on surface electrocardiography were excluded. Bipolar and unipolar electrograms were filtered at 10 to 400 Hz and 1 to 240 Hz, respectively. Electrogram duration was manually measured from the initial sharp deflection of the EGM until the beginning of the decay potential at 400 mm/s speed as described by Cassidy et al.[12] Fractionated potentials are defined as electrogram amplitude less than 0.5 mV and a duration more than 133 ms; and late potentials are defined as intracardiac electrograms with any component recorded after the inscription of the latest surface QRS activity as defined by Cassidy et al.[12] Electrogram amplitude was recorded as the difference between the highest and lowest deflections of a stable contact signal.

3D reconstruction of CEP-MDCT and registration of EAM

The endocardial and epicardial borders of the left ventricle, the endocardial border of the right ventricle, and aortic cusps and root borders were contoured using ADAS-VT software (Galgo Medical, Barcelona, Spain). Contours were manually traced in the short-axis plane, complemented by two-chamber and coronal planes to differentiate blood pool and pericardial fat. The contouring process is illustrated in Figure 1A-B. After the contouring process, areas that contained implantable cardioverter-defibrillator (ICD) generator or lead artifacts were manually excluded as shown in the Figure 1C. Images were then 3D reconstructed and exported to CARTO3 software for registration using the CartoMERGE module of CARTO3 software (Biosense Webster, Diamond Bar, CA). Initial registration was performed by matching one fixed reference point with the His bundle or the right aortic cusp (Figure 2). This was followed by adjusting the registration based on locations of aortic cusps, aorta, right ventricle, apex, and mitral annulus. Merged images were reimported to ADAS-VT software. Using an internal function, the ADAS-VT software divided the myocardium into 9 equal layers which follow the shape of endocardial and epicardial layer. Layers are made of triangle meshes, and segmental attenuation of each layer was calculated from triangles using the trilinear interpolation method reflecting the immediate vicinity of the voxel. For the study, the average attenuation of the first 5 layers calculated by ADAS-VT was defined as the endocardial attenuation, and the average attenuation of the last 4 layers was defined as the epicardial attenuation. The average attenuation of all 9 layers was defined as the full-thickness myocardial attenuation. EAM points were projected using the ADAS-VT software to the closest point on the CT shell. The attenuation of each projected EAM point was then calculated using trilinear interpolation. In addition, site specific wall thickness was automatically calculated from the registered image. Several patients presented with calcifications in scar areas. The attenuation of areas with calcification is expected to be very high and would produce a non-linear association between attenuation and voltage. Given the paucity of such sites, and to simplify the association to a linear model, segments with image attenuation >200 HU were excluded from analysis. The median distance of EAM points to the LV endocardium was 6.27 mm with an (IQR 4.83–7.96 mm)

Local conduction velocity analyses

Local CV analyses were performed according to a previously validated methodology.[13–16] The local CV of each EAM point was defined as the average of the CV between that point and 5 adjacent points along the activation front, where the CV between each pair of points was defined as the linear distance between the points divided by the difference in activation times. To avoid the inclusion of CV measurements in a different direction than that of activation propagation, points with difference in local activation time <5 ms from the index point were excluded from the CV calculation for that index point. Using this methodology, the CV at all EAM points was automatically calculated with a custom calculating script written in Python (https://www.python.org)[13] The CV and full thickness attenuation data for each EAM point was then exported for analyses as panel data clustered by patient.

Statistical Analyses

Continuous variables are expressed as mean ± standard deviation (SD) or median ± 25th to 75th percentiles, and categorical variables are expressed as absolute values and percentages. To examine the association between attenuation and other variables, a ultilevel random effects linear regression model clustered by patient was used. As bipolar, unipolar, and CV variables do not follow a normal distribution curve, logarithmic conversion was performed when they were the dependent variable. If logarithmic conversion was performed, the correlation coefficient was recognized to reflect the ratio of change instead of actual arithmetic change. Thus, all the correlations coefficients between independent variable and logarithmically converted dependent variable were expressed as percent change in the dependent variable. All statistical analyses were performed using STATA 15 (Stata Corp, College Station, TX).

Results

Patient characteristics

The cohort consisted of 14 patients (median age 62.5 (IQR 58.3–67.5), 79% male) with post-infarct ventricular tachycardia. Median duration from preoperative CEP-MDCT to ablation was 1 (IQR 0–2) day. All patients underwent endocardial mapping and ablation, and 1 patient had additional epicardial mapping and ablation. Of 14 patients, 12 (86%), had a previously implanted ICD or CRT-D system. Three patients (21%) were found to have calcified myocardium in low voltage areas. Patient characteristics have been summarized in Table 1.

Association of Conduction Velocity with Image Attenuation

A total of 4103 EAM points were collected during baseline rhythm. Of these, 414 (10%) points were excluded due to localization within a high attenuation CEP-MDCT image region, representing lead artifact or calcification. The remaining 3689 EAM points and corresponding myocardial attenuation were used for analysis. The mean electrogram duration on EAM was 79.6 ± 23.4 ms. The mean CV on EAM was 0.53 ± 0.40 m/s (0.21 between-patient SD and 0.34 within-patient SD). The mean bipolar voltage on EAM was 1.46 ± 1.83 mV (0.65 between-patient and 1.76 within-patient SD). The mean unipolar voltage on EAM was 5.07 ± 3.32 mV (2.11 between-patient and 2.91 within-patient SD). On CEP-MDCT imaging, the mean attenuation for endocardium, epicardium, and full-thickness myocardium was 70.9 ± 41.1 HU, 59.9 ± 46.6 HU and 65.9 ± 39 HU, respectively. The mean LV wall-thickness was 6.83 ± 3.17 mm. There were 94 (2.6%) fragmented potentials and 307 (8.3%) late potentials.

In the multi-level, random effects linear regression model, clustered by patient, CV was associated with full-thickness myocardial attenuation (2.9% decrease in CV per 10 HU decrease in attenuation, 95% CI: 2.3%−3.5%, $p<0.001$) and with the endocardial attenuation (2.2% drop in local CV per 10 HU decrease, 95% CI: 1.6%−2.7%; $p<0.001$). When adjusted for wall thickness, the association between full-thickness attenuation and local CV was maintained; every 10 HU decrease resulted in 2.6% drop in local CV (95% CI 1.9%−3.2%, $p<0.001$). The association of local CV and full-thickness attenuation for each patient is

illustrated in Figure 3. Local CV was also associated with myocardial wall thickness (2.4% decrease in local CV per 1 mm thinning in wall, 95% CI 1.6%−3.2%; P<0.001) and it was strongly associated with bipolar and unipolar voltage, as every 1 mV decrease in bipolar or unipolar voltage resulted in a 12.3% (95% CI 11.1%−13.5%, p<0.001) or 6.9% (95% CI; 6.1%−7.6%, p<0.001) drop in local CV, respectively. The association between attenuation on CEP-MDCT, local CV and voltage measurements has been graphically depicted in Figure 4.

Full-thickness attenuation and voltage association

In the multi-level, random effects linear regression model, clustered by patient, bipolar electrogram amplitude was positively associated with full-thickness attenuation on CEP-MDCT (7.5% drop in bipolar electrogram amplitude for every 10 HU decrease, 95%CI: 6.5% – 8.5%, p<0.001) and endocardial attenuation (5.9% drop in bipolar electrogram amplitude for every 10 HU decrease, 95% CI: 5% −6.9%; p<0.001). When adjusted for wall thickness, bipolar voltage amplitude remained associated with full-thickness attenuation (5.5% drop in electrogram amplitude per 10 HU decrease in attenuation, 95% CI: 4.5–6.6; p<0.001). Unipolar electrogram amplitude was similarly associated with full-thickness myocardial attenuation (4.2% drop in electrogram amplitude per 10 HU decrease, 95%CI: 3.8%−4.7%; p<0.001). Bipolar voltage amplitude was also associated with wall thickness (10.5% decrease in amplitude per 1 mm thinning, 95% CI: 9.2%−11.8%; P<0.001).

Multivariable regression analysis, clustered by patient, revealed a significant inverse association between EGM duration and full-thickness attenuation with every 10 HU decrease associated with 0.85 ms increase in duration (95%CI: −1.04 - −0.65, p<0.001). EGM duration was also inversely associated with myocardial wall thickness (r=−0.39, 95%CI: - 0.64 – −0.14; p <0.001).

Fragmented potentials were significantly associated with full-thickness attenuation on CEP-MDCT (OR 0.89 per 10 HU increase, 95% CI: 0.85 – 0.93; p<0.001), and more likely to correspond the areas with low CV (OR 0.005, per 1 m/s increase in CV, 95% CI: 0.001 – 0.02, p<0.001). Similarly, late potentials tended to be found in areas with decreased full-thickness attenuation (OR 0.90 per 10 HU increase in attenuation, 95%CI: 0.87 – 0.93, p<0.001), and with low CV (OR 0.16 per 1 m/s increase in CV, 95% CI: 0.10 – 0.26, p<0.001).

Discussion

The major findings from this study are that: (1) Myocardial hypoattenuation on CEP-MDCT is associated with reduced CV and decreased bipolar and unipolar electrogram amplitudes, and (2) Hypoattenuated CEP-MDCT areas are more likely to show increased electrogram duration, fragmented potentials, and late potentials.

CEP-MDCT to augment substrate-guided ventricular tachycardia ablation

Previous animal and clinical studies have confirmed an association between post-infarct scar geometry on cardiac imaging and histological analysis.[17] Similar to MRI, CEP-MDCT has been shown to demonstrate scar accurately following myocardial infarction.[18] In the setting of post-infarct VT, local abnormal ventricular electrograms either co-localize to, or are

found in the immediate vicinity of, regions with wall thinning on CEP-MDCT.[9] Interestingly, heterogeneity in wall thickness measured by CEP-MDCT has been proposed as an indicator of arrhythmogenic substrate.[19]

Measurement of attenuation provides a complimentary method for feature extraction from CEP-MDCT images for detection of post-infarct scar. Attenuation measurements from first-pass perfusion MDCT are constant with narrow standard deviation in healthy volunteers and have been shown to detect areas of ischemia, acute and chronic myocardial infarction with high sensitivity and specificity.[20–22] Previous studies have illustrated that delayed enhancement MDCT image findings mirror those of late gadolinium enhancement (LGE) MRI in identification of the scar substrate for VT.[23] Similarly, hypoattenuation during contrast perfusion appears to be indicative of scar, likely because of reduced vascularity in fibrotic regions.[23, 24] The size of hypoperfused regions on CEP-MDCT and hyperintense regions in LGE-MRI are similar.[23] Although prior studies from our group and others have focused on the value of LGE-MRI, scar surrogates on MDCT including wall thickness and hypoattenuation offer improved generalizability to clinical use and higher spatial resolution. Prior studies have shown that hypoperfusion, end-systolic or end-diastolic wall thickness, and wall motion abnormalities correlate with abnormal voltage amplitude.[7, 8, 25] Our study applied a point-by-point approach, quantitatively confirming the association between bipolar and unipolar electrogram abnormalities with full-thickness attenuation on first-pass CEP-MDCT. The present study expands upon prior findings by uncovering an association between electrogram duration and hypoattenuation. Additionally, we showed that critical VT circuit surrogates, such as fragmented potentials and late potentials, more likely in the areas with hypoattenuation and low conduction velocity.

Association of conduction velocity with hypoattenuation

Following myocardial infarction, local CV is altered due to disruption of normal myocardial architecture and development of areas of fibrosis, which provide barriers to conduction. Therefore, it stands to reason that local CV should associate with abnormal bipolar voltage in ventricular tissue. In addition, up to 20% of patients with chronic ischemic cardiomyopathy develop lipomatous metaplasia within infarcted regions.[26–28] These regions exhibit low bipolar and unipolar voltage[7] as well as low CV.[29] In the present study,we demonstrated that local CV is lower in areas with decreased hypoattenuation on first pass CEP-MDCT. It is likely that we detected a spectrum of fibrofatty deposition in areas with decreasing attenuation, which was associated with decreased CV. Local CV was also strongly and independently associated with previously established scar surrogates such as bipolar voltage and wall thickness. Furthermore, fragmented and late potentials tended to be found in areas with low local CV.

Addition of local CV data to the established scar surrogate measures could potentially improve patient outcomes in RFCA. Because regions with decreased local CV are likely to act as critical substrates for re-entrant tachycardias, demonstration of local CV association with hypoattenuated areas further strengthens the utility of CEP-MDCT for substrate-guided catheter ablation.

Study Limitations

This is a single center observational study with a limited sample size, which may have resulted in selection bias and limited generalizability of results. Future studies with more patients would allow for adjustment of potential confounders that were not measured in this study. Twelve patients had either an ICD system implanted. Lead artifacts were usually limited to the septum and were excluded using the imaging software, but artifacts may have impacted the evaluation of septal attenuation. Exclusion of calcified areas in several patients may have limited the evaluation of the scarred areas in the ventricle. The median registration accuracy in our study is 6 mm which might have impacted our ability to assess the scar area. Even with careful segmentation, small amounts of endoluminal contrast or periventricular fat tissue might sometimes be included within myocardial contours. This unintentional error would manifest as misclassification of myocardium as diseased or normal myocardium; thus, we do not expect it to result in differential bias. To reduce the likelihood of ectopy during mapping, and to ensure the collection of quality contact signals, a standard ablation catheter was used rather than a multipolar catheter. As a result, contact quality is likely higher but point density is relatively reduced compared to studies that utilize high density mapping catheters. Reduced point density might affect CV determination, particularly in dense score regions. However, a minority of points (7.6 %) were acquired from dense scar cores, and a sensitivity analysis that excluded dense scar core points (<0.1 mV) did not affect the magnitude or direction of association between attenuation and CV.

Conclusion

Hypoattenuated areas detected by CEP-MDCT were associated with low local CV and low bipolar and unipolar electrogram amplitudes as detected by EAM, in post-infarct VT patients. Regions with low CV as identified by low attenuation on CEP-MDCT are likely to serve as important VT substrates in patients with post-infarct VT. Incorporation of CEP-MDCT and local CV maps may complement EAM mapping and result in new strategies for RFCA in patients with post-infarct VT.

Acknowledgments

Funding: The study was funded through NIH grant R01HL116280 to Dr. Nazarian. The contents do not necessarily represent the views of the National Institutes of Health. The study was also supported by funds from the Jeffrey and Jo Ann Dickson Cardiac Electrophysiology Fund.

Disclosures: Dr. Nazarian is a consultant for St Jude Medical, Siemens, Biosense Webster, ImriCor, and CardioSolv. Dr. Nazarian also serves as PI for research funding from Biosense Webster, Imricor, and Siemens.

References

1. Sapp JL, Wells GA, Parkash R, et al. Ventricular tachycardia ablation versus escalation of antiarrhythmic drugs. N Engl J Med 2016;375:111–121 [PubMed: 27149033]
2. Fahmy TS, Wazni OM, Jaber WA, et al. Integration of positron emission tomography/computed tomography with electroanatomical mapping: A novel approach for ablation of scar-related ventricular tachycardia. Heart Rhythm 2008;5:1538–1545 [PubMed: 18984529]
3. Sasaki T, Miller CF, Hansford R, et al. Myocardial structural associations with local electrograms: A study of postinfarct ventricular tachycardia pathophysiology and magnetic resonance-based noninvasive mapping. Circ Arrhythm Electrophysiol 2012;5:1081–1090 [PubMed: 23149263]

4. Sasaki T, Hansford R, Zviman MM, Kolandaivelu A, Bluemke DA, Berger RD, Calkins H, Halperin HR, Nazarian S. Quantitative assessment of artifacts on cardiac magnetic resonance imaging of patients with pacemakers and implantable cardioverter-defibrillators. Circ Cardiovasc Imaging 2011;4:662–670 [PubMed: 21946701]
5. Cury RC, Nieman K, Shapiro MD, et al. Comprehensive assessment of myocardial perfusion defects, regional wall motion, and left ventricular function by using 64-section multidetector ct. Radiology 2008;248:466–475 [PubMed: 18641250]
6. Tian J, Jeudy J, Smith MF, et al. Three-dimensional contrast-enhanced multidetector ct for anatomic, dynamic, and perfusion characterization of abnormal myocardium to guide ventricular tachycardia ablations. Circ Arrhythm Electrophysiol 2010;3:496–504 [PubMed: 20657032]
7. Sasaki T, Calkins H, Miller CF, Zviman MM, Zipunnikov V, Arai T, Sawabe M, Terashima M, Marine JE, Berger RD, Nazarian S, Zimmerman SL. New insight into scar-related ventricular tachycardia circuits in ischemic cardiomyopathy: Fat deposition after myocardial infarction on computed tomography--a pilot study.Heart Rhythm 2015;12:1508–1518 [PubMed: 25814415]
8. Esposito A, Palmisano A, Antunes S, Maccabelli G, Colantoni C, Rancoita PMV,Baratto F, Di Serio C, Rizzo G, De Cobelli F, Della Bella P, Del Maschio A. Cardiac ct with delayed enhancement in the characterization of ventricular tachycardia structural substrate: Relationship between ct-segmented scar and electro-anatomic mapping. JACC Cardiovasc Imaging 2016;9:822–832 [PubMed: 26897692]
9. Komatsu Y, Cochet H, Jadidi A, et al. Regional myocardial wall thinning at multidetector computed tomography correlates to arrhythmogenic substrate in postinfarction ventricular tachycardia: Assessment of structural and electrical substrate. Circ Arrhythm Electrophysiol 2013;6:342–350 [PubMed: 23476043]
10. Nayyar S, Wilson L, Ganesan A, Sullivan T, Kuklik P, Young G, Sanders P, Roberts-Thomson KC. Electrophysiologic features of protected channels in late postinfarction patients with and without spontaneous ventricular tachycardia. J Interv Card Electrophysiol 2018;51:13–24 [PubMed: 29236200]
11. Ng FS, Kalindjian JM, Cooper SA, Chowdhury RA, Patel PM, Dupont E, Lyon AR, Peters NS. Enhancement of gap junction function during acute myocardial infarction modifies healing and reduces late ventricular arrhythmia susceptibility. JACC Clin Electrophysiol 2016;2:574–582 [PubMed: 27807593]
12. Cassidy DM, Vassallo JA, Buxton AE, Doherty JU, Marchlinski FE, Josephson ME. The value of catheter mapping during sinus rhythm to localize site of origin of ventricular tachycardia. Circulation 1984;69:1103–1110 [PubMed: 6713614]
13. Fukumoto K, Habibi M, Ipek EG, et al. Association of left atrial local conduction velocity with late gadolinium enhancement on cardiac magnetic resonance in patients with atrial fibrillation. Circ Arrhythm Electrophysiol 2016;9:e002897 [PubMed: 26917814]
14. Kistler PM, Sanders P, Fynn SP, Stevenson IH, Spence SJ, Vohra JK, Sparks PB, Kalman JM. Electrophysiologic and electroanatomic changes in the human atrium associated with age. J Am Coll Cardiol 2004;44:109–116 [PubMed: 15234418]
15. John B, Stiles MK, Kuklik P, Chandy ST, Young GD, Mackenzie L, Szumowski L, Joseph G, Jose J, Worthley SG, Kalman JM, Sanders P. Electrical remodelling of the left and right atria due to rheumatic mitral stenosis. Eur Heart J 2008;29:2234–2243 [PubMed: 18621772]
16. Miyamoto K, Tsuchiya T, Narita S, Yamaguchi T, Nagamoto Y, Ando S, Hayashida K, Tanioka Y, Takahashi N. Bipolar electrogram amplitudes in the left atrium are related to local conduction velocity in patients with atrial fibrillation. Europace 2009;11:1597–1605 [PubMed: 19910315]
17. de Bakker JM, van Capelle FJ, Janse MJ, Wilde AA, Coronel R, Becker AE, Dingemans KP, van Hemel NM, Hauer RN. Reentry as a cause of ventricular tachycardia in patients with chronic ischemic heart disease: Electrophysiologic and anatomic correlation. Circulation 1988;77:589–606 [PubMed: 3342490]
18. Lardo AC, Cordeiro MA, Silva C, et al. Contrast-enhanced multidetector computed tomography viability imaging after myocardial infarction: Characterization of myocyte death, microvascular obstruction, and chronic scar. Circulation2006;113:394–404 [PubMed: 16432071]

19. Ghannam M, Cochet H, Jais P, Sermesant M, Patel S, Siontis KC, Morady F, Bogun F. Correlation between computer tomography-derived scar topography and critical ablation sites in postinfarction ventricular tachycardia. J Cardiovasc Electrophysiol 2018;29:438–445 [PubMed: 29380921]

20. Stanton CL, Haramati LB, Berko NS, Travin MI, Jain VR, Jacobi AH, Burton WB, Levsky JM. Normal myocardial perfusion on 64-detector resting cardiac ct. J Cardiovasc Comput Tomogr 2011;5:52–60 [PubMed: 21185253]

21. Ramsey BC, Fentanes E, Choi AD, Branch KR, Thomas DM. Myocardial assessment with cardiac ct: Ischemic heart disease and beyond. Curr Cardiovasc Imaging Rep 2018;11:16 [PubMed: 29963220]

22. Choe YH, Choo KS, Jeon ES, Gwon HC, Choi JH, Park JE. Comparison of mdct and mri in the detection and sizing of acute and chronic myocardial infarcts. Eur J Radiol2008;66:292–299 [PubMed: 17686598]

23. Gerber BL, Belge B, Legros GJ, Lim P, Poncelet A, Pasquet A, Gisellu G, Coche E,Vanoverschelde JL. Characterization of acute and chronic myocardial infarcts by multidetector computed tomography: Comparison with contrast-enhanced magnetic resonance. Circulation 2006;113:823–833 [PubMed: 16461822]

24. Buecker A, Katoh M, Krombach GA, Spuentrup E, Bruners P, Gunther RW, Niendorf T, Mahnken AH. A feasibility study of contrast enhancement of acute myocardial infarction in multislice computed tomography: Comparison with magnetic resonance imaging and gross morphology in pigs. Invest Radiol 2005;40:700–704 [PubMed: 16230902]

25. Misra S, Zahid S, Prakosa A, Saju N, Tandri H, Berger RD, Marine JE, Calkins H, Zipunnikov V, Trayanova N, Zimmerman SL, Nazarian S. The field of view of mapping catheters quantified by electrogram associations with radius of myocardial attenuation on contrast-enhanced cardiac computed tomography. Heart Rhythm 2018

26. Ichikawa Y, Kitagawa K, Chino S, Ishida M, Matsuoka K, Tanigawa T, Nakamura T, Hirano T, Takeda K, Sakuma H. Adipose tissue detected by multislice computed tomography in patients after myocardial infarction. JACC Cardiovasc Imaging 2009;2:548–555 [PubMed: 19442939]

27. Ahn SS, Kim YJ, Hur J, Lee HJ, Kim TH, Choe KO, Choi BW. Ct detection of 1subendocardial fat in myocardial infarction. AJR Am J Roentgenol 2009;192:532–537 [PubMed: 19155421]

28. Zafar HM, Litt HI, Torigian DA. Ct imaging features and frequency of left ventricular myocardial fat in patients with ct findings of chronic left ventricular myocardial infarction. Clin Radiol 2008;63:256–262 [PubMed: 18275865]

29. Pouliopoulos J, Chik WW, Kanthan A, Sivagangabalan G, Barry MA, Fahmy PN, Midekin C, Lu J, Kizana E, Thomas SP, Thiagalingam A, Kovoor P. Intramyocardial adiposity after myocardial infarction: New implications of a substrate for ventricular tachycardia. Circulation 2013;128:2296–2308 [PubMed: 24036606]

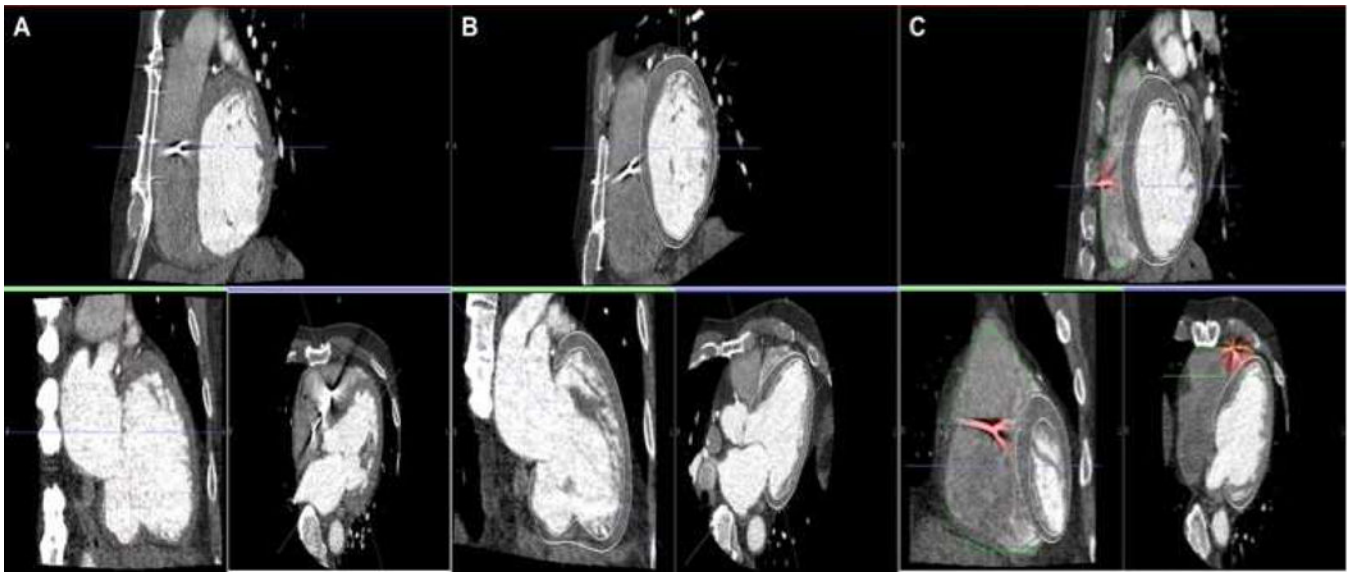

Figure 1. CEP-MDCT images, segmentation, artifact exclusion

CEP-MDCT segmentation, and extraction of lead artifact areas. Panel A shows CEP-MDCT in coronal, axial and sagittal views. Panel B Shows representative cardiac contouring in each image plane. Panel C shows lead artifact exclusion (highlighted as red).

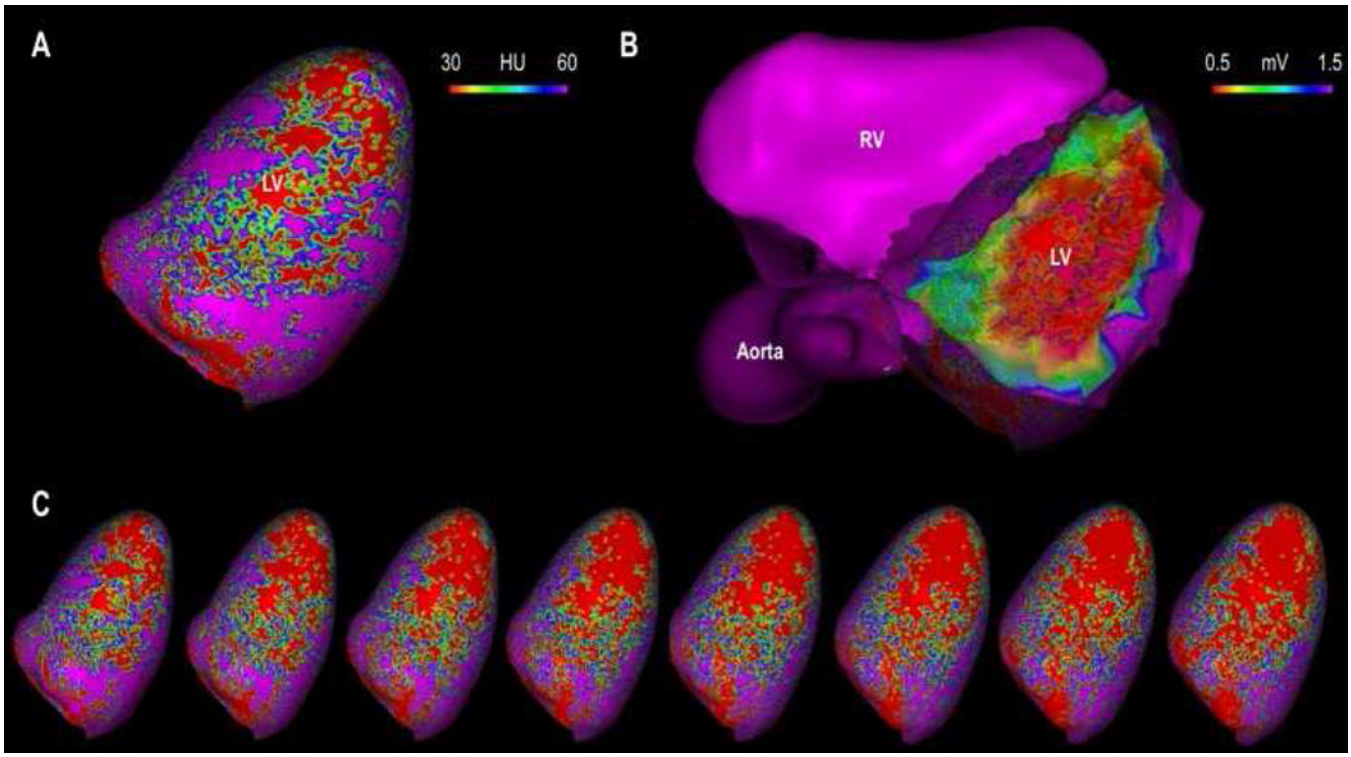

Figure 2. Image registration

The figure illustrates the process for co-registration of the electroanatomic map to CEP-MDCT reconstructions using landmarks (His bundle, or right aortic cusp) followed by visual and surface registration. Panel A shows a 3D reconstructed CT shell with attenuation color coded for the 10% depth (endocardial) layer of the myocardium. Panel B shows the EAM registered to CEP-MDCT with a transparent CT reconstruction shell for comparison to Panel A. Panel C shows sequential (right to left) CT reconstructions representing attenuation from the 20%, 30%, 40%, 50%, 60%, 70%, 80%, and 90% (epicardial) myocardial depths.

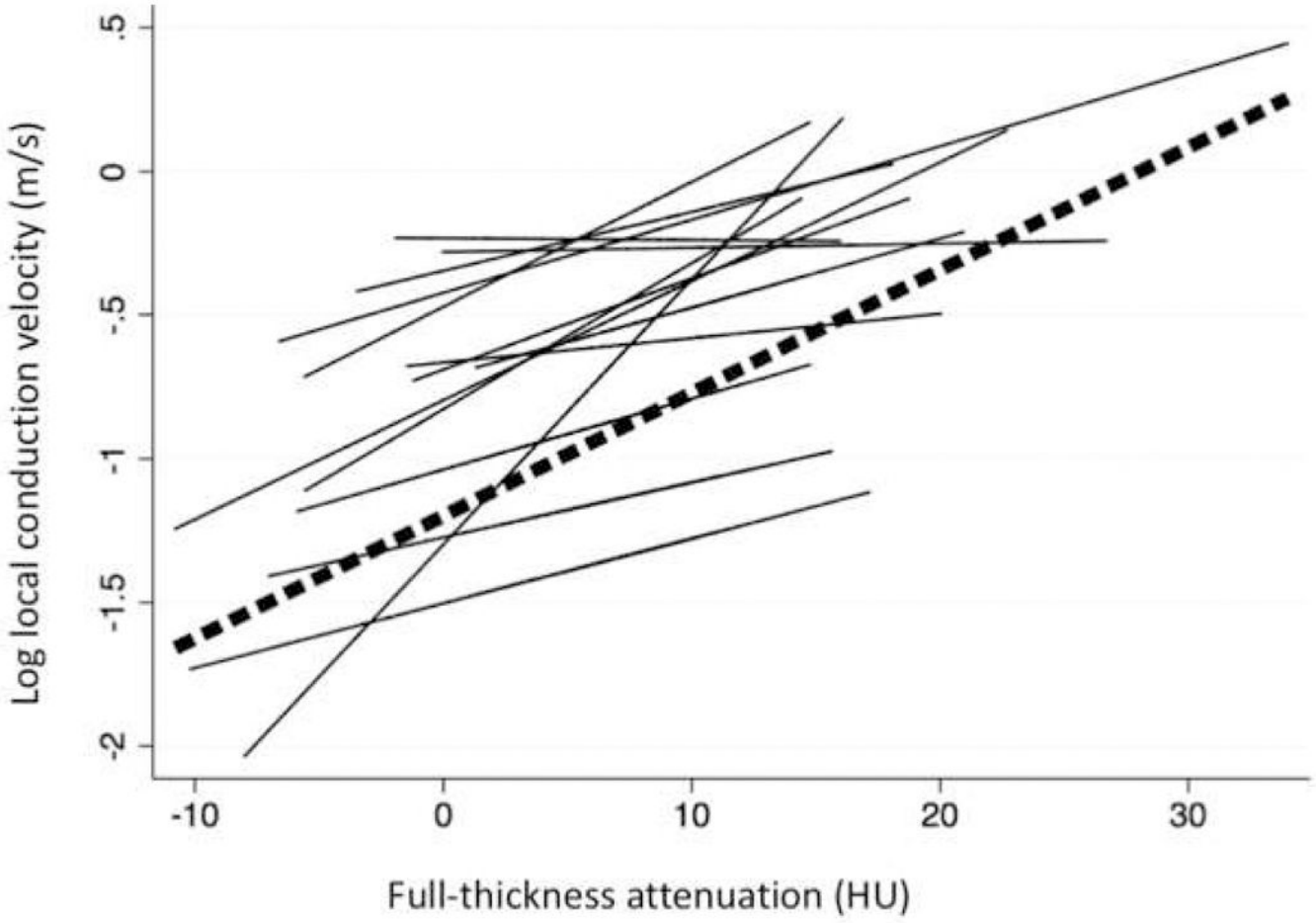

Figure 3. Spaghetti Plot of local CV versus attenuation among individual patients

Straight lines represent individual regression fits for each patient for the association between full-thickness attenuation and local CV. The dashed line represents the overall association between full-thickness attenuation and local CV.

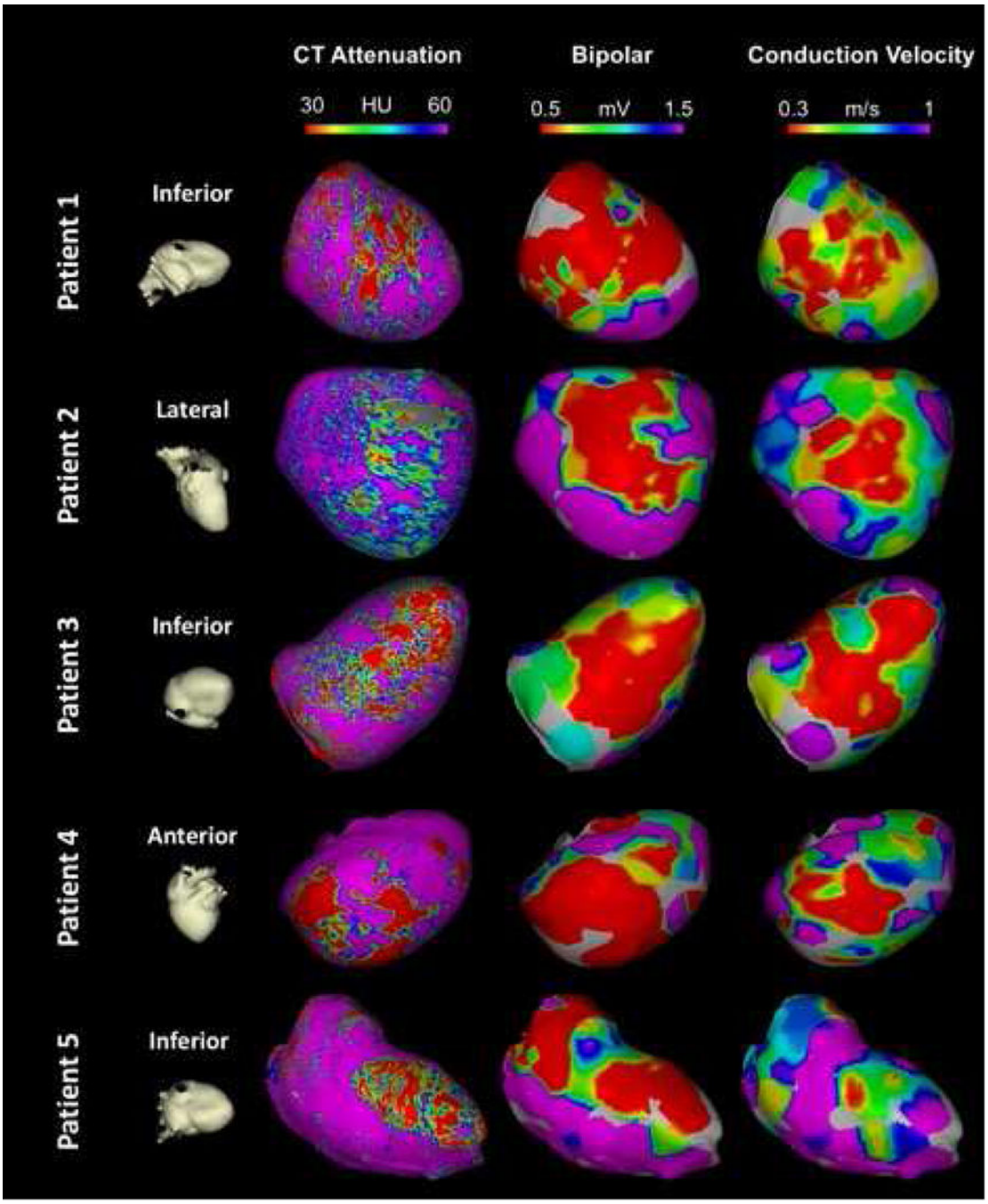

Figure 4. Comparison of Conduction velocity, CEP-MDCT attenuation maps, and Electroanatomic maps in 5 representative patients

Each row represents a different patient. The first column shows cardiac orientation for the subsequent images in each row. The images in the second column represent endocardial attenuation maps (10% layer). The Gray area in patient 2 has been excluded due to ICD artifact. Images in the third column represent bipolar voltage maps projected on the 3D reconstructed shell from MDCT. Finally, images in the fourth column represent the local CV map projected on the 3D reconstructed shell from MDCT. Of note, the resolution of Panel A

is 1194 point/cm^3, whereas the resolution of panels B and C is limited by the electroanatomic mapping density at 1.08 point/cm^3.

Table 1.

Patient Characteristics

Median Age[1]	62.5 (58.3–67.5)
PentaRAY[2]	3 (21%)
Thermocool SF[2]	11 (79%)
Male[2]	11 (79%)
Single chamber – ICD[2]	3 (21%)
Dual chamber – ICD[2]	5 (36%)
CRT-D[2]	4 (29%)
Median duration from CT to ablation[1]	1 (0–2)
VT recurrence in 5 years of follow-up[2]	7 (50%)

[1]Continuous variables are expressed as median (interquartile range).

[2]Categorical variables are expressed as absolute values and percentages